World Applied Sciences Journal 7 (8): 1006-1015, 2009
ISSN 1818-4952

Frequency Response Analysis in Power Transformer for Detection of Winding Short-circuit using Quasi-static Finite Element and Circuit-based Method

[1]M.R. Barzegaran, [1]M. Mirzaie, [2]A. Shayegani Akmal

[1]Department of Electrical Engineering, Babol University of Technology, Babol, Iran
[2]Department of Electrical Engineering, Tehran University, Tehran, Iran

Abstract: Detecting and removing minor faults in power transformer winding is essential because minor faults may develop and lead to major faults and finally irretrievable damages occur. In this paper in order to detect the position of short-circuit in the winding, frequency response of the input impedance of a power transformer is analyzed. Common short-circuits are categorized and the results are compared, then the behavior of frequency response due to disk-disk short-circuit is investigated. To increase the accuracy of analysis, innovative approach in finite element analysis is offered. This approach termed Electromagnetic quasi-static considers both magnetic and electric characteristics of power transformer. Simulation is fulfilled by interconnecting between finite element analysis and circuit-based model for employing short-circuit.

Key words: Electromagnetic . circuit-based model . fault . finite element analysis . power transformer . quasi static . sweep frequency response analysis

INTRODUCTION

NOWADAYS reliability is an inevitable part of power system studies and operation, due to significant increase in the number of industrial electrical consumers. Power transformer is one of the major and critical elements in power system in the area of reliability issue, since their outage may result in costly and time-consuming repair and replacement. For each transformer, windings and insulations are the most critical elements economically and technically, so highly protection should be considered for them.

The main fault that occurs in a transformer is internal short circuit through the winding, which may lead to serious damage in winding on transformer including winding deformation, interruption or even the explosion of the transformer because of overheating the insulating liquid which is usually oil. Consequently, winding need to be frequently checked to avoid major damages.

In order to distinguish fault in winding, many methods are suggested which can be classified into two major categories: experimental methods and simulation-based methods. It is obvious that the experimental detection of internal fault is essential and important, but applying long term and high cost experimental tests to find the best detection method is impossible because of the transformer cost. Therefore, Due to economical limitations in experimental tests, Simulation has been considered as the best approach to introduce innovative analysis, to compare with other methods and finally, to select the best method in the area of fault detection in transformers. A comprehensive review of the best methods introduced so far is presented in following.

In experimental analysis, in [1] Al-Ammar *et al.* improved the fault detection sensitivity through impulse test. He utilized short time Fourier transforms for better clarification of the differences between various kinds of faults. Also M. Naderi [2] presented detection and modeling incipient faults including short circuit between disks during impulse test and using wavelet transform for better comparison. Ryder [3] identified various internal faults in winding through frequency response analysis. He used correlation coefficient for comparing faults through wide band frequency. Kim *et al.* [4] improved frequency response analysis by using a signal processing technique. He determined the defective coil with synthetic spectral analysis.

As a numerical analysis, in [5], a comparison between experimental results and numerical simulation results of the transfer function is presented for a medium-voltage transformer winding. A wavelet transform-based method is offered by Singh and Rao [6]. The proposed method is applied for investigation of trivial faults and predicting the actual fault location in the winding.

Corresponding Author: Mr. Mohammadreza Barzegaran, Department of Electrical Engineering, Babol University of Technology, Babol, Iran

In lumped section method, Sahoo [7] investigated the localization of discrete faults (i.e. short-circuit of turns) through sweeping along frequency. Also Islam and Ledwich [8] employed the same approach and analyzed the results through transfer function.

As an example of distributed-parameter s-domain method, in literature [9], a new mathematical-based method is developed. The results are swept along high frequencies. It is shown that the frequency resonances obtained by the proposed method are sensitive to short-circuits.

Finite Element method has been considered in many researches toward less error and higher similarity with experimental results. In [10] analysis of transformer performance under internal short-circuit is considered. It is demonstrated the deviation of axial and redial forces during short-circuit in windings. Faiz *et al*. [11] utilized the same approach and also investigated normalized flux density along the winding. He also discriminate short-circuit and inrush current using FEA. O.A.Mohammad [12] employed discrete wavelet transform through with FEA in modeling and characterizing the internal faults. This survey is done in time-domain. S. Liu *et al*. [13] presented the FE-based phase variable model of single-phase distribution transformers with internal short-circuit faults. They utilized a defined equivalent magnetizing current in identifying the characteristics of internal short-circuit.

In this paper, finite element method is employed as one of the most accurate simulation method with novel techniques that make the analysis more accurate. The finite element method including principles and electromagnetic quasi-static analysis are discussed in section II. Procedure in detecting the location of the fault using circuit-based model is explained in section III. Section IV consists of simulation results and comprehensive interpretation of the results respectively. Conclusion is located in section V, lastly.

FINITE ELEMENT METHOD

In this section principle of coupled field-circuit FEM and the approach which is used in this paper are discussed. Some novelty are used which is explained too.

Finite element analysis (FEA) is a very sophisticated tool widely used by engineers, scientists and researchers to solve engineering problems arising from various physical fields such as electromagnetic, thermal, structural, fluid flow, acoustic and others. Currently the finite element method is clearly the dominant numerical analysis method for the simulation of physical field distributions, with success not paralleled by any other numerical technique. In essence, the finite element method finds the solution to any engineering problem that can be described by a finite set of spatial partial derivative equations with appropriate boundary and initial conditions. It is used to solve problems for an extremely wide variety of static, steady state and transient engineering applications from diverse markets such as automotive, aerospace, nuclear, biomedical, etc.

The finite element method has a solid theoretical foundation. It is based on mathematical theorems that guarantee an asymptotic increase of the accuracy of the field calculation towards the exact solution as the size of the finite elements used in the solution process decreases. For time domain solutions the spatial discretization of the problem must be refined in a manner coordinated with the time steps of the calculation according to estimated time constants of the solution (such as magnetic diffusion time constant).

Finite Element Analysis solves the electromagnetic field problems by solving Maxwell's equations in a finite region of space with appropriate boundary conditions and, when necessary, with user-specified initial conditions in order to obtain a solution with guaranteed uniqueness. In order to obtain the set of algebraic equations to be solved, the geometry of the problem is discretized automatically into tetrahedral elements. All the model solids are meshed by mesh operation. The assembly of all tetrahedra is referred to as the finite element mesh of the model or simply the mesh. Inside each tetrahedron, the unknowns characteristic for the field being calculated are represented as polynomials of second order. Thus, in regions with rapid spatial field variation, the mesh density needs to be increased for good solution accuracy. More explanation is expressed in [14, 15].

According to the previous works, most of them used electric or magnetic solution, but it this paper a new solution method is used that fully coupled magnetic and electric solution that is named electromagnetic quasi-static whick also simplify solving along frequencies.

Principle of coupled field-circuit approach: The magnetic field inside the power transformer is directed by the following nonlinear partial differential equations:

$$\nabla \times \left(\nu \nabla \times \mathbf{A} \right) = \mathbf{J} \tag{1}$$

$$\nabla \cdot \sigma \left(\frac{\partial \mathbf{A}}{\partial t} + \nabla V \right) = 0 \tag{2}$$

where **A** is the magnetic vector potential, **J** is the total current density, ν is the magnetic reluctivity, V is the

electric scalar potential and s is the electric conductivity.

The current in the circuit domain is governed by the following set of mesh equation:

$$\begin{aligned}\left[\mathbf{E}_m\right]=&\left[R_m\right]\left[\mathbf{I}_m\right]+\left[L_m\right]\frac{d}{dt}\left[\mathbf{I}_m\right]\\&+\left[\frac{1}{C_m}\right]\int\left[\mathbf{I}_m\right]dt+\left[\frac{1}{G_m}\right]\left[\mathbf{I}_{g_m}\right]\end{aligned}\tag{3}$$

where E_m represent the vector of voltage sources in each electric mesh m I_m is the vector of current in each mesh. R_m L_m, C_m and G_m are the matrix of resistances, inductances, capacitances and conductance to ground, respectively. I_{gm} represents the current that leaks to the ground as a result of insulation ageing or etc.

Equations (1) and (2) are coupled with the equation (3) and solved simultaneously. The external circuit connections are used to describe the electrical connectivity between the conducting regions, external loads and power supplies. When a fault occurs, the magnetic flux distribution is fundamentally altered as well as the current in the circuit domain. But, the transformer terminal behavior still satisfies (1-3). Thus obtaining the faulty transformer behavior is achieved by solving these equations.

Principle of electromagnetic quasi-static analysis: Electromagnetic quasi-static analysis is valid under the assumption that $\partial\mathbf{D}/\partial t = 0$. This implies that Maxwell's equations can be rewritten in the following manner.

$$\nabla\times\mathbf{H}=\mathbf{J}=\sigma(\mathbf{E}+\nu\times\mathbf{B})+\mathbf{J}^e\tag{4}$$

$$\nabla\times\mathbf{E}=-\frac{\partial\mathbf{B}}{\partial t},\nabla\cdot\mathbf{B}=0,\nabla\cdot\mathbf{J}=0,\nabla\cdot\mathbf{D}=\rho\tag{5}$$

Here $\mathbf{J}^\theta$ is an externally generated current density and ν is the velocity of the conductor. The crucial criterion for the quasi-static approximation to be valid is that the currents and the electromagnetic fields vary slowly. This means that the dimensions of the structure in the problem need to be small compared to the wavelength. Note that **B** and **E** are used uniquely in magnetic or electric solution respectively, but are fully coupled here.

Using the definitions of the potentials,

$$\mathbf{B}=\nabla\times\mathbf{A}\tag{6}$$

$$\mathbf{E}=-\nabla\mathbf{V}-\frac{\partial\mathbf{A}}{\partial t}\tag{7}$$

and the constitutive relation $\mathbf{B} = \mu 0(\mathbf{H} + \mathbf{M})$, Ampère's law can be rewritten as

$$\sigma\frac{\partial\mathbf{A}}{\partial t}+\nabla\times(\mu_0^{-1}\nabla\times\mathbf{A}-\mathbf{M})-\sigma\nu\times(\nabla\times\mathbf{A})+\sigma\nabla\mathrm{V}=\mathbf{J}^e\tag{8}$$

The equation of continuity, which is obtained by taking the divergence of the above equation, gives us the equation

$$-\nabla\cdot\left(\sigma\frac{\partial\mathbf{A}}{\partial t}-\sigma\nu\times(\nabla\times\mathbf{A})+\sigma\nabla\mathrm{V}-\mathbf{J}^e\right)=0\tag{9}$$

These two equations give us a system of equations for the two potentials **A** and V.

$$-\nabla\cdot(-\sigma\mathbf{v}\times(\nabla\times\mathbf{A})+\sigma\nabla\mathrm{V}-\mathbf{J}^e=0\tag{10}$$

$$\nabla\times(\mu_0^{-1}\nabla\times\mathbf{A}-\mathbf{M})-\sigma\mathbf{v}\times(\nabla\times\mathbf{A})+\sigma\nabla\mathrm{V}=\mathbf{J}^e\tag{11}$$

The term $\sigma\mathbf{V}\times(\nabla\times\mathbf{A})$ represents the current generated motion with a constant velocity in a static magnetic field, $\mathbf{J}^B = \sigma\mathbf{v}+\mathbf{B}^e$. Similarly the term $-\sigma\nabla\mathbf{V}$ represents a current generated by a static electric field, $\mathbf{J}^E = \sigma\mathbf{E}^e$. When $\mathbf{J}^B = 0$, including $\mathbf{J}^E$ in the external current results in the equation

$$\nabla\times(\mu_0^{-1}\nabla\times\mathbf{A}-\mathbf{M})=\tilde{\mathbf{J}}^e\tag{12}$$

with $\tilde{\mathbf{J}}^e=\mathbf{J}^e+\mathbf{J}^E$. This equation can be solved independently from the other equation.

The electric and magnetic potentials are not uniquely defined from the electric and magnetic fields through (6) and (7).

Introducing two new potentials

$$\tilde{\mathbf{A}}=\mathbf{A}+\nabla\Psi\tag{13}$$

$$\tilde{\mathrm{V}}=\mathrm{V}-\frac{\partial\Psi}{\partial t}\tag{14}$$

gives the same electric and magnetic fields:

$$\mathbf{E}=-\frac{\partial\mathbf{A}}{\partial t}-\nabla\mathrm{V}=-\frac{\partial(\tilde{\mathbf{A}}-\nabla\Psi)}{\partial t}-\nabla(\tilde{\mathrm{V}}+\frac{\partial\Psi}{\partial t})=-\frac{\partial\tilde{\mathbf{A}}}{\partial t}-\nabla\tilde{\mathrm{V}}\tag{15}$$

$$\mathbf{B}=\nabla\times\mathbf{A}=\nabla\times(\tilde{\mathbf{A}}-\nabla\Psi)=\nabla\times\tilde{\mathbf{A}}\tag{16}$$

The variable transformation of the potentials is called a gauge transformation. To obtain a unique solution you need to choose the gauge, that is, put

constraints on Ψ that make the solution unique. Another way of expressing this additional condition is to put a constraint on $\nabla\cdot\mathbf{A}$. **A** vector field is uniquely defined up to a constant if both $\nabla\cdot\mathbf{A}$ and $\nabla\times\mathbf{A}$ are given. This is called Helmholtz's theorem. One particular gauge is the Coulomb gauge given by the constraint $\nabla\cdot\mathbf{A}=0$.

When using assemblies with interface pairs, it might also be necessary to activate an equation fixing a gauge. This has to be done when vector elements are coupled over a pair and the meshes on each side are incompatible. The gauge is the Coulomb gauge for Magneto-statics and Quasi-statics for electric and induction currents. Quasi-statics for induction currents uses other equations when fixing the gauge. These equations are shown below, where the first equation is for time-harmonic problems and the second equation is for transient problems.

$$\nabla\cdot\mathbf{J}=0$$

$$\nabla\cdot(\sigma\mathbf{A})=0 \tag{17}$$

In the frequency-response case, Ampere's equation includes the displacement current:

$$\nabla\times\mathbf{H}=\mathbf{J}=\sigma(\mathbf{E}+\nu\times\mathbf{B})+j\omega\mathbf{D}+\mathbf{J}^{e} \tag{18}$$

In the transient case, the inclusion of this term would lead to a second-order equation in time, but in the harmonic case there are no such complications. Using the definition of the electric and magnetic potentials, the system of equations becomes

$$-\nabla.\begin{pmatrix}(j\omega\sigma-\omega^2\varepsilon_0)\mathbf{A}-\sigma\nu\times(\nabla\times\mathbf{A})+\\(\sigma+j\omega\varepsilon_0)\nabla V-(\mathbf{J}^{e}+j\omega\mathbf{P})\end{pmatrix}=0 \tag{19}$$

$$(j\omega\sigma-\omega^2\varepsilon_0)\mathbf{A}+\nabla\times(\mu_0^{-1}\nabla\times\mathbf{A}-\mathbf{M})-\sigma\nu\times(\nabla\times\mathbf{A})$$
$$+(\sigma+j\omega\varepsilon_0)\nabla V=(\mathbf{J}^{e}+j\omega\mathbf{P})$$

The constitutive relation $\mathbf{D}=\varepsilon_0\mathbf{E}+\mathbf{P}$ has been used for the electric field.

It can be obtained a particular gauge that reduces the system of equation by choosing $\Psi=-jV/\omega$ in the gauge transformation. This gives

$$\tilde{\mathbf{A}}=\mathbf{A}-\frac{j}{\omega}\nabla V,\ \tilde{V}=0 \tag{20}$$

Because $\tilde{V}$ vanishes from the equations, the second equation in (19) is only needed, i.e. $(\sigma+j\omega\varepsilon_0)\nabla V$ is eliminated in (19).

Working with $\tilde{\mathbf{A}}$ is often the best option when it is possible to specify all source currents as external currents $\mathbf{J}^{e}$ or as surface currents on boundaries. More information is explained in [16].

CIRCUIT-BASED MODEL

As it is mentioned in previous part, analysis is performed with interfacing between finite element method and circuit-based method. The process consists of estimating transformer's parameters such as inductances, resistances and capacitances between disks and also between disks to ground. Then, parameters are put into the circuit-based model. This innovative method spends considerably less time in analysis in comparison with finite element analysis (FEA). Performing different types of short-circuits in FEA is too time-consuming. Also employing and changing load and supply is difficult and limited in finite element analysis.

Solution in this model is based on s-domain (Laplace). The model is derived from long-line model can be used in detecting the location and number of shorted turns by using several cascaded blocks. This is discussed in following.

Consider the model shown in Fig. 2 represents the assumed equivalent circuit for each coil turn. Theoretically, an infinite number of such equivalent circuits can be cascade interconnected in order to model the whole winding. This model has considerable accuracy in comparison with other simulation methods [7, 8].

In order to perform short-circuit, an equivalent resistance block (R) is cascade interconnected with shorted turns (block S) that is shown in Fig. 2. Non short-circuited coils are simulated in block X, Y.

For employing turn to turn short-circuit, Rs must be zero and for employing turn to ground short-circuit Rp must be zero.

All blocks in Fig. 2 are solved by long-line model formulas. For instance, short-circuited block (s) that actually represents the number of short-circuited turns has $[ABCD]_S$ matrix. The matrix is as follows.

$$\left[ABCD\right]_S=\begin{bmatrix}\cosh(\gamma ls) & Z_C\sinh(\gamma ls)\\ \dfrac{\sinh(\gamma ls)}{Z_C} & \cosh(\gamma ls)\end{bmatrix} \tag{21}$$

The equivalent characteristic impedance Z_C and propagation constant γ of each section are given by:

$$Z_C=\sqrt{\frac{z(s)}{y(s)}} \tag{22}$$

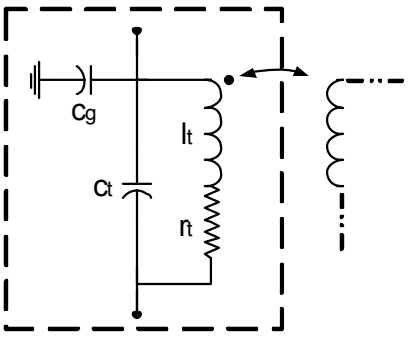

Fig. 1: Equivalent model for each transformer disk

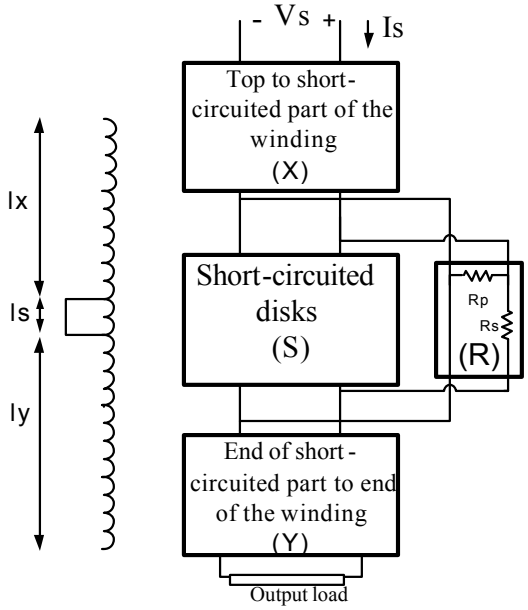

Fig. 2: Equivalent cascaded model

$$\gamma = \sqrt{z(s)y(s)}$$

where $z(s)$ and $y(s)$ are the input impedance and admittance of the equivalent model that is shown in Fig. 1

In section R that performs short-circuit, the $[ABCD]_R$ are as follow

$$\left[ABCD\right]_R = \begin{bmatrix} 1 & R_S \\ \frac{1}{R_P} & \frac{R_S + R_P}{R_P} \end{bmatrix} \quad (23)$$

Each two section are connected together by cascading them to form an equivalent [ABCD] and the result will be cascaded with the other section to form the whole model. The two parallel sections S and R are done first. So, cascading these two sections to form an equivalent T with the following $[ABCD]_T$ founded as follows:

$$A_T = \frac{A_S B_R + A_R B_S}{B_S + B_R} \quad (24)$$

$$B_T = \frac{B_S B_R}{B_S + B_R} \quad (25)$$

$$C_T = C_S + C_R + \frac{(A_S - A_R) + (D_R - D_S)}{B_S + B_R} \quad (26)$$

$$D_T = \frac{A_S B_R + A_R B_S}{B_S + B_R} \quad (27)$$

The overall matrix can be solved as follows

$$\begin{bmatrix} A_X & B_X \\ C_X & D_X \end{bmatrix} \times \begin{bmatrix} A_T & B_T \\ C_T & D_T \end{bmatrix} \times \begin{bmatrix} A_Y & B_Y \\ C_Y & D_Y \end{bmatrix} = \begin{bmatrix} A_K & B_K \\ C_K & D_K \end{bmatrix} \quad (28)$$

Since receiving end voltage and current are related by the load impedance $Z_L = R_L + Sl_L$, the input impedance seen from the input is found to be:

$$Z_{in} = \frac{Z_L A_K + B_K}{Z_L C_K + D_K} \quad (29)$$

The amplitude and phase angle of this impedance will be the parameters on which the suggested fault recognition procedure is based.

To check the validity of this model, a test is performed. First, output impedance is set to zero (Z_L = 0). Then for simulating not faulted winding both R_S and R_P are taken as 8. The derived input impedance will be as follows

$$Z_{in} = Z_C \tanh(\gamma l) \quad (30)$$

The magnitude and phase of this state are represented in Fig. 3, 4 respectively. The results of the cascaded model under this case will not be affected when changing either ls or ly or both at the same time, as expected, since no faults exist.

SIMULATION RESULTS AND DISCUSSION

The proposed simulation is based on a three phase actual power transformer. Power transformer is selected because of a high possibility of damages in power transformer rather than smaller distribution transformer. Transformer is modeled in details as much as possible to yield the maximum accuracy. Many details are considered consist of pressboards, gaps between layers of all disks, papers, details of materials and all other fragments. The transformer main parameters are as

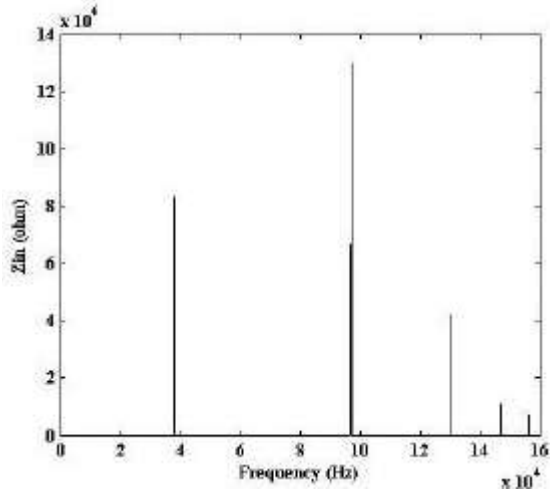

Fig. 3: Frequency response of input impedance (amplitude) when Rs,Rp=8 and shorted output ($Z_L = 0$)

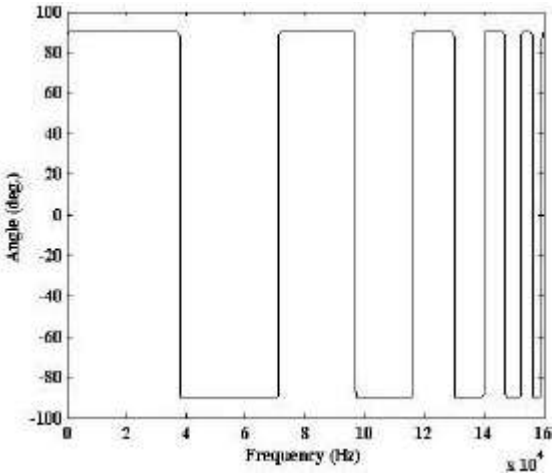

Fig. 4: Frequency response of input impedance (phase) when Rs,Rp=8 and shorted output ($Z_L = 0$)

follows: 30 MVA, 63 KV/ 20 KV, Ynd1 and 50 Hz. Details of the transformer are reported in Appendix.

In this section, first primitive results of finite element analysis are represented and then results of classified faults are shown.

As it was anticipated, flux density (B) is usually between 0.7 and 1.7 tesla in the core at the frequency of 50 Hz. Presenting flux density in magnetic analysis in finite element method is limited to the intrinsic variables and flux density changes due to these variables. These variables are frequency and angle in permanent magnetic simulation and time in transient simulation. Here, flux density depicted in 50 Hz and is shown in Fig. 5. Asymmetry of the flux density is due to instantaneous plotting in special phase angle of flux density. For better resolution, front view of the transformer is illustrated in Fig. 5.

Simulation with a lot of triangles in mesh operation is selected to increase accuracy, although it will take longer time for analysis. While the number of triangles is varied between 95000 and 135000, the energy error and delta energy are less than 1%. Also, the number of triangles is changed for different types of fault. Each analysis has been done in 47 hours which then is increased considerably because of the frequency response analysis.

Studying the types of short-circuit: In this section, it is proposed to investigate and compare the results of common short-circuit in transformer winding. Many types of short-circuit may occur in the winding, but some of them are more common according to IEEE standard C57.140 [17].

One of the main types of short-circuit in transformer winding is turn to turn or disk to disk short-circuit. This type of short-circuit occurs because of the aging of the winding insulation. Insulation aging may lead to reduce oil break-down voltage and/or even paper erosion. Moreover, as a result of vibration in transportation and maintenance, the standard distance between disks and other components in transformer may change. This will cause abnormal distribution of field in coil and short-circuit may occur. The disk to disk short-circuit may not be detected instantly and the transformer works for a long period, but damages due to the short-circuit cause hot spot and accelerate aging of papers, oil and other material close to short-circuit region.

Another type of short-circuit is turn or disk to ground. As a result of persistence of partial discharge due to the moisture or other factors, amount of air increases in oil and oil break-down voltage may decrease. Consequently, the efficient distance between disks and ground decreases and short-circuit between disk and ground occurs in long period of time. In addition to partial discharge, deformation of winding due to transportation or assembly of transformer has impact in happening this kind of short-circuit.

Short-circuit between two turns and ground is considered as the third type of common faults. This kind of short-circuit may occurs due to persistence of the first state (disk-disk short-circuit). Opposite current which flows between shorted disks in turn-turn short-circuit make hot spot in the area. Therefore oil break-down voltage decreases and short-circuit to the ground may occur.

Most types of short-circuits are included into these three states. For instance, short-circuit between lead to the ground can be included into the second state.

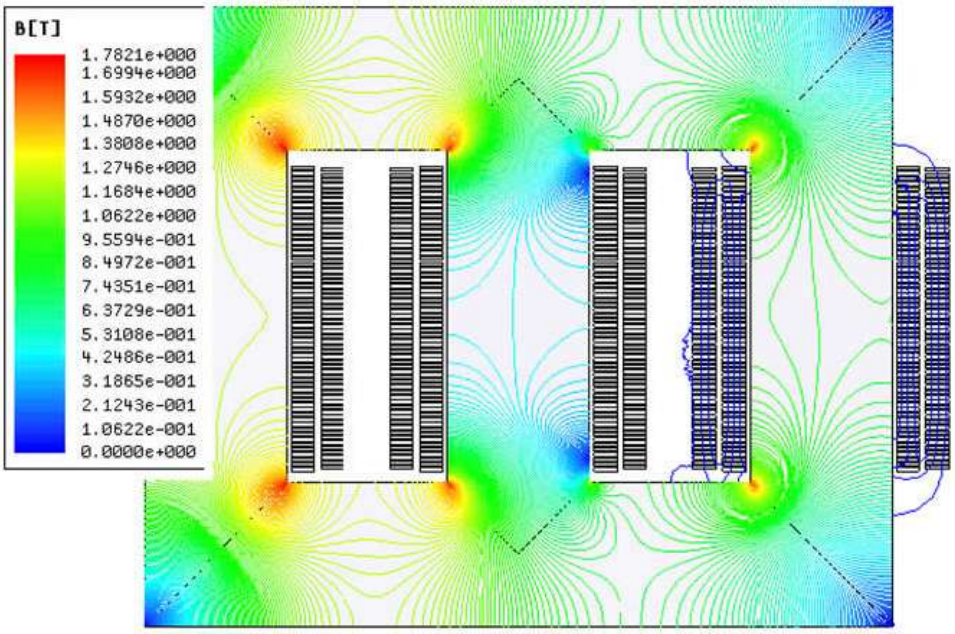

Fig. 5: Frontal view of flux density distribution in the core of the proposed transformer at 50 Hz

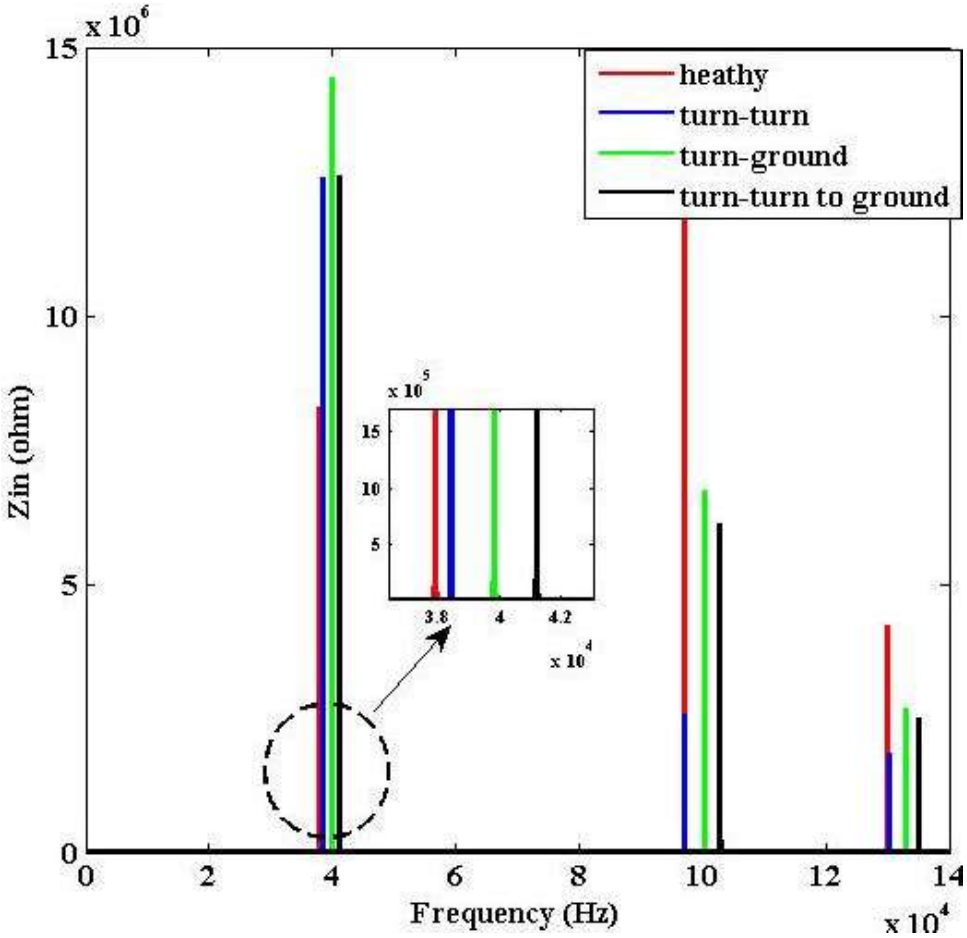

Fig. 6: Frequency response of input impedance (amplitude) in various types of short-circuits in shorted output

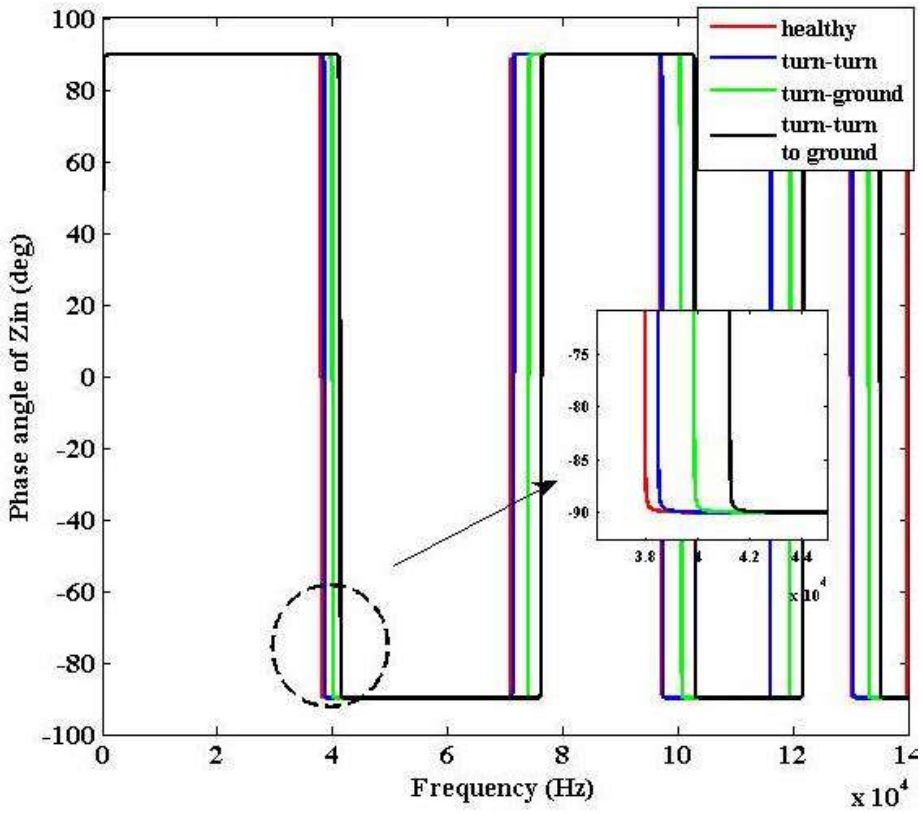

Fig. 7: Frequency response of input impedance (angle) in various types of short-circuits in shorted output

Comparison of these three states are represented in Fig. 6.

According to Fig. 6, movement of resonances in frequency axis due to the various types of short-circuits is slight, although deviation of amplitude is considerable.

Deviation of the location of the first resonance in frequency axis between healthy and turn-turn state is slight. This is because of shorting only one or two turns. So the amplitude of current may not varied considerably. On the other hand, the changes in turn-ground short-circuit is significant that is because of shorting many turns. Therefore recognition of this kind of short-circuit is easier compared to the former type. For more comprehensive recognition, phase angle of input impedance is analyzed and demonstrated in Fig. 7.

Studying the location of short-circuit: After studying the types of short-circuit, identifying the position of short-circuit along winding is proposed. For brevity, the position of the disk-disk short-circuit is investigated.

Changes in the position of resonance along frequency band (axis X) due to short-circuit is slight, so for better recognition, estimation of DR (deviation of resonance) is proposed

Table 1: Deviation of resonance coefficient (DR) in disk-disk short-circuit

Position of short-circuit	DR of the first resonance	DR of the second resonance	DR of the third resonance
Disks 1-2	1.582	1.151	0.763
Disks 5-6	1.556	0.898	0.383
Disks 11-12	1.428	0.369	0.030
Disks 23-24	1.017	0.133	0.763
Disks 35-36	0.524	1.070	0.0307
Disks 47-48	0.157	0.696	0.764

$$DR = \frac{f_f - f_h}{f_f} \times 100 \quad (31)$$

In equation (31) f_h is the frequency of resonance in healthy state and f_f is the frequency of resonance in faulty state.

Table 1 shows the value of DR of first, second and the third resonances of disk-disk short-circuit in several points along winding.

According to Table 1, as it was mentioned before changing the position of resonance along frequency band is slight in turn-turn or disk-disk short-circuit. Table 1 also represented that by moving the position of short-circuit along winding, the first resonance moves

Table 2: Transformer data

Symbol	Quantity	Value
S	Nominal Power	30 MVA
V_{HV}	High voltage winding (primary side)	63 KV line
V_{LV}	Low voltage winding (secondary side)	20 KV line
	Type of Connection	Star-delta
	Cooling type	ONAN-ONAF
	Number of LV turn (each limb)	232
	Number of HV1 turn (each limb)	352
	Number of HV2 turn (each limb)	70
	Number of HV3 turn (each limb)	63
	Tap setting	normal
	Core steel type	M5

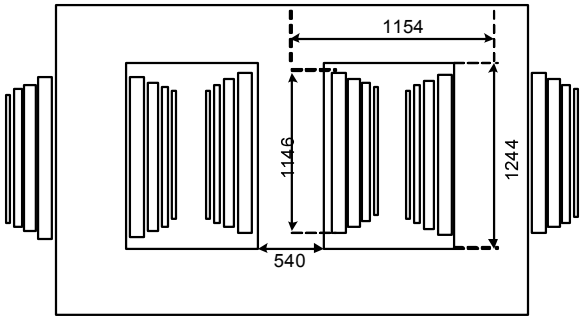

Fig. 8: Primitive geometry details of analyzed power transformer (dimensions are in mm)

orderly along frequency axis but the second and the third resonances move disorderly. So it is recommended to use the first resonance for studying and detecting short-circuits in transformer winding.

Since the DR is positive in disk-disk short-circuit, it can be concluded in this kind of short-circuit resonance move from the healthy state to right in frequency axis (higher frequencies). Moreover, by moving the position of short-circuit to top of the winding, resonance get closer to the healthy state in frequency axis.

CONCLUSION

In this paper electromagnetic quasi-static analysis is used for achieving accurate simulation. Parameters of transformer are estimated by means of finite element analysis and utilized in circuit-based model and the input impedance is calculated in wide band frequency. In addition to classifying and analyzing main types of short-circuit, frequency response of disk-disk short-circuit state is investigated in several points the HV winding.

According to the simulation results, the first resonance of input impedance due to short-circuit moves orderly but the second and the third resonances move disorderly so for determining the position of short-circuit in winding investigating the first resonance of input impedance is suggested. In addition, deviation of resonances along frequencies due to disk-disk short-circuit is less than disk-ground and disk-disk to ground short-circuits.

Appendix

Some designing parameters of the employed transformer are mentioned in Table 2 and the geometry is drawn in Fig. 8.

The analysis is investigated in lower tap. HV2 and HV3 are omitted in lower tap.

REFERENCES

1. Al-Ammar, G. Karady and H. Jin Sim, 2008. Novel Technique to Improve the Fault Detection Sensitivity in Transformer Impulse Test. IEEE Trans. Power Delivery, 23 (2): 717-725.
2. Naderi, M., G. Gharepatian and M. Abedi, 2008. Modeling and Detection of Transformer Internal Incipient Fault during Impulse Test. IEEE Trans. Dielect. Electr. Insul., 15 (1): 284-291.
3. Ryder, S.A., 2003.Diagnosing Transformer Faults Using Frequency Response Analysis. IEEE Electrical Insulation Magazine, 19 (2): 16-22.
4. Kim, J. and B. Park and S. Jeong, 2005. Fault Detection of a Power Transformer Using an Improved Frequency-Response Analysis. IEEE Trans. Power Delivery, 20 (1): 169-178.
5. Florkowski, M. and J. Furgal, 2003. Detection of Transformer Winding Deformation Based on the Transfer Function-Measurements and Simulation. J. Meas. Sci. Technol., 14: 1986-1992.
6. Rao, M.R. and B.P. Singh, 2001. Detection and Localization of inter turn fault in the HV winding of a power transformer using wavelets. IEEE Trans. Dielect. Electr. Insul., 8 (4): 652-657.
7. Satish, L. and S.K. Sahoo, 2009. Locating Fault in a Transformer Winding: An Experimental Study. Electrical Power System Research, 79: 89-97.
8. Islam, S. and G. Ledwich, 1996. Locating Transformer Faults through Sensitivity Analysis of High Frequency Modeling Using Transfer Function Approach, Conference record of the 1996 IEEE international symposium of electrical insulation, Montreal, Canada, pp: 89-97.
9. Saied, M. and A.S. Alfuhaid, 2004. Frequency Response of two-winding transformers obtained by a distributed-parameter s-domain method. Journal of Electric Power Components and Systems, 32 (8): 5888, 755-766.

10. Kumbhar, G.B. and S.V. Kulkarni, 2007. Analysis of Short-Circuit Performance of Split-Winding Transformer Using Coupled Field-Circuit Approach. IEEE Trans. Power Delivery, 22 (2): 936-943.
11. Faiz, J., B.M. Ebrahimi and T. Noori, 2008. Three- and Two-Dimensional Finite-Element Computation of Inrush Current and Short-Circuit Electromagnetic Forces on Windings of a Three-Phase Core-Type Power Transformer. IEEE Trans. Magnetics, 44 (5): 590-597.
12. Abed, N.Y. and O.A. Mohammed, 2007. Modeling and Characterization of Transformers Internal Faults Using Finite Element and Discrete Wavelet Transforms. IEEE Trans. Magnetics, 43 (4): 1425-1428.
13. Liu, S., Z. Liu and O.A. Mohammed, 2007. FE-Based Modeling of Single-Phase Distribution Transformers with Winding Short Circuit Faults. IEEE Trans. Magnetics, 43 (4): 1841-1844.
14. Anastasis, C. Polycarpou and Constantine Balanis, 2006. Introduction to the Finite Element Method in Electromagnetic, Morgan and Claypool Publisher.
15. Liu, G.R. and S.S. Quek, 2003. The finite element method: A practical course, butterworth-heinermann.
16. Zijad Haznadar and Željko Štih, 2000. Electromagnetic fields, waves and numerical methods, IOS Press.
17. IEEE Guide for the Evaluation and Reconditioning of Liquid Immersed Power Transformers. IEEE STD C57.140 2006.